

Surrogate-Guided Quantum Discovery in Black-Box Landscapes with Latent-Quadratic Interaction Embedding Transformers

Saisubramaniam Gopalakrishnan, Dagnachew Birru

Philabs, Quantiphi

India, USA

{gopalakrishnan.saisubramaniam,dagnachew.birru}@quantiphi.com

Abstract

Discovering configurations that are both high-utility and structurally diverse under expensive black-box evaluation and strict query budgets remains a central challenge in data-driven discovery. Many classical optimizers concentrate on dominant modes, while quality-diversity methods require large evaluation budgets to populate high-dimensional archives. Quantum Approximate Optimization Algorithm (QAOA) provides distributional sampling but requires an explicit problem Hamiltonian, which is unavailable in black-box settings. Practical quantum circuits favor quadratic Hamiltonians since higher-order interaction terms are costly to realize. Learned quadratic surrogates such as Factorization Machines (FM) have been used as proxies, but are limited to pairwise structure. We extend this surrogate-to-Hamiltonian approach by introducing a Latent-Quadratic Interaction Embedding Transformer (QET) that models higher-order variable dependencies via self-attention and projects them into a valid Positive Semi-Definite quadratic form compatible with QAOA. This enables diversity-oriented quantum sampling from learned energy landscapes while capturing interaction structure beyond pairwise terms. We evaluate on risk discovery for enterprise document processing systems against diverse classical optimizers. Quantum-guided samplers achieve competitive utility while consistently improving structural diversity and exclusive discovery. FM surrogates provide stronger early coverage, whereas QET yields higher-fidelity surrogate landscapes and better extreme-case discovery. QET-QAOA methods recover roughly twice as many structurally tail-risk outliers as most classical baselines and identify an exclusive non-overlapping fraction ($\approx 4\text{--}5\%$) of high-utility configurations not found by competing methods. These results highlight Latent-Quadratic Interaction embedding with self-attention as an effective mechanism for learning higher-order interaction structure and projecting it into quadratic surrogate Hamiltonians for quantum-assisted black-box discovery.

Keywords

Quantum Machine Learning, Surrogate Modeling, Black-Box Optimization, QAOA, Transformer-based Surrogates

1 Introduction

Discovering configurations that are simultaneously high-utility and structurally diverse in complex black-box landscapes is a fundamental challenge in data-driven science and engineering. This need for high-coverage discovery spans domains as diverse as *de novo* molecular design [6], financial stress testing [5], and the reliability assurance of Intelligent Document Processing (IDP) systems [3], where the objective is rarely a single global optimum but rather a diverse portfolio of high-performing solutions. This setting is especially

critical in validation workflows, where uncovering multiple distinct failure modes is essential for robust assurance. However, such problems are typically governed by expensive black-box oracles and strict query budgets, rendering exhaustive search infeasible.

Classical approaches rely primarily on population-based heuristics, yet they exhibit well-known limitations under tight evaluation budgets. Evolutionary and swarm-based methods effectively exploit local information but often suffer from mode collapse, converging to narrow clusters around dominant basins of attraction [2]. Quality-Diversity (QD) methods such as MAP-Elites explicitly enforce behavioral diversity through archive-based illumination [22, 24], but their archive-filling dynamics are frequently sample-inefficient in high-dimensional spaces, often requiring orders of magnitude more evaluations than are available in industrial testing regimes. Bayesian Optimization (BO) and reinforcement learning (RL) methods are query-efficient for sequential decision-making, but are typically formulated to optimize scalar objectives or expected return, and require additional novelty or entropy regularization to support diverse solution set discovery [20, 29]. As a result, there remains a gap between query-efficient optimization and principled discovery of structurally diverse high-utility configurations.

Quantum optimization offers a complementary mechanism for maintaining solution diversity through probabilistic sampling over an energy landscape. However, algorithms such as the Quantum Approximate Optimization Algorithm (QAOA) [4] require an explicit problem Hamiltonian, which is not directly accessible in black-box settings. Learned quadratic surrogates such as Factorization Machines (FM) [26] partially address this gap by modeling pairwise interactions, and have recently been coupled with quantum optimizers in black-box design pipelines [31]. Nevertheless, such models are limited in their ability to represent higher-order dependencies and are typically applied to optimization rather than diverse discovery.

To address these limitations, we propose the *Latent-Quadratic Interaction Embedding Transformer (QET)*, a surrogate-guided quantum discovery framework that learns a quadratic proxy Hamiltonian directly from observational data. QET employs a Transformer encoder with self-attention to model higher-order dependencies among decision variables, and projects the learned interactions into a valid positive semi-definite (PSD) quadratic form compatible with Ising/QUBO representations. This surrogate Hamiltonian is then used within QAOA at low alternating-operator depth, enabling the quantum circuit to function as a structured diversity-oriented sampler rather than a traditional ground-state optimizer. By adjusting circuit parameters and mixing operators, the sampler concentrates probability mass around multiple low-energy basins while preserving multi-modal coverage. We empirically evaluate

the framework on high-dimensional reliability testing of enterprise Intelligent Document Processing (IDP) systems, which serves as a representative High-dimensional Expensive Problem (HEP) [37] setting. The search space is combinatorial, the oracle is computationally costly, and the resulting risk landscape is fragmented and non-differentiable. The underlying structure of assembling discrete document components to optimize a black-box risk score makes this benchmark representative of a broader class of other scientific discovery problems.

Our contributions are as follows:

- **Latent Proxy Hamiltonian Learning:** We introduce a novel surrogate architecture *Latent-Quadratic Interaction Embedding Transformer (QET)* that bridges deep learning and quantum. Unlike standard FM limited to fixed pairwise interactions, QET employs a self-attention mechanism to capture complex, higher-order dependencies in the black-box objective. We introduce a projection layer that maps these latent embeddings onto a valid, Positive Semi-Definite (PSD) quadratic form, effectively constructing a realizable Ising Hamiltonian from observational data.
- **Quantum Diversity Sampling:** We reframe the role of QAOA from ground state optimization to diversity sampling. We demonstrate that by driving the ansatz with the learned QET proxy, the induced wavefunction leverages quantum superposition to simultaneously populate distinct low-energy basins, effectively bypassing the mode collapse typical of greedy classical heuristics.
- **Structural Exclusivity & Outlier Quantification:** We validate the framework on a document processing risk discovery benchmark against 10 state-of-the-art solvers and their variants. We demonstrate that QET achieves superior predictive fidelity ($R^2 \approx 0.84$), through set-theoretic analysis it isolates a distinct utility subspace (4–5% of yield exclusive to the union of other baselines), and alongside FM-surrogate, it ranks amongst the top in discovering tail 1% edge cases, making it an important surrogate mechanism for robust quantum-based discovery.

2 Related Work

We situate our contributions at the intersection of budget-constrained black-box optimization, diversity-driven search, and quantum-assisted machine learning. This section contrasts our framework with existing classical heuristics, classical surrogate and policy learning approaches, and prior work in quantum for optimization.

2.1 Optimizers and Diversity-Driven Discovery

The challenge of identifying sets of solutions that are both high-performing and structurally distinct (termed Quality-Diversity (QD) or Illumination) is central to complex systems discovery. Standard population-based heuristics, such as Genetic Algorithms (GA) [11] and Particle Swarm Optimization (PSO) [16], prioritize gradient-free exploitation but frequently suffer from *mode collapse*. These methods often converge to a single basin of attraction, leaving structurally distinct high-utility regions unexplored [2]. To mitigate this, QD algorithms like MAP-Elites [22] and Novelty Search with Local Competition (NSLC) [18] explicitly mandate diversity by

maintaining archives of solutions indexed by behavioral descriptors. While QD methods excel at coverage, they are notoriously *sample inefficient*, typically requiring hundreds of thousands of evaluations ($> 10^5$) to illuminate high-dimensional feature spaces [24]. This renders them impractical for industrial settings governed by expensive black-box oracles. Our framework bridges this gap: by using QET to learn the *latent topology* of the landscape, we construct a surrogate that enables the solver to mimic diversity-seeking behavior of QD methods, but with the sample efficiency of optimizers.

2.2 Surrogate-Based and Policy Optimization

For expensive black-box functions, Bayesian Optimization (BO) [30] remains the standard for sample efficiency. By utilizing probabilistic surrogates such as Gaussian Processes (GP) or Tree-structured Parzen Estimators (TPE) [1], BO guides the search toward promising regions. However, standard kernels (e.g., Matérn or Hamming) often struggle to capture complex, non-local variable dependencies in high-dimensional combinatorial spaces. To address this, Factorization Machines (FM) [26] and their neural variants, such as DeepFM [9] and Attentional Factorization Machines (AFM) [35], have emerged as powerful surrogates. Unlike linear models, FMs explicitly model second-order interactions and have been successfully applied to material design and discovery [12, 17].

Parallel to surrogate modeling, Deep Reinforcement Learning (DRL) has been adapted for combinatorial optimization, treating the search as a sequential decision process. Policy gradient methods, specifically REINFORCE [34] and Proximal Policy Optimization (PPO) [28], have shown promise in learning constructive heuristics. However, these methods are typically data-hungry and require exploration to stabilize the policy gradient in sparse-reward environments, making them less suitable for strictly budget-constrained discovery compared to surrogate-based approaches.

2.3 Quantum-Assisted Learning and Sampling

The integration of quantum solvers with classical surrogates, e.g. FMQA [17], has demonstrated that learned FM weights can be directly mapped to Quadratic Unconstrained Binary Optimization (QUBO) formulations for Quantum Annealers (QA) [13]. However, existing FMQA literature focuses strictly on scalar minimization to collapse the system to a single global optimum. Our work diverges by repurposing this pipeline for diversity sampling. We leverage the variational gate-based QAOA [4] algorithm to sample from a multi-modal wavefunction, effectively addressing the budgeted discovery [8] problem where finding a diverse portfolio of candidates is superior to point-convergence. Furthermore, while standard QAOA relies on unconstrained transverse field mixing, our framework aligns with the Quantum Alternating Operator Ansatz (QAOA+) [10] by utilizing interaction-aware mixing from the learned QUBO to preserve domain constraints, ensuring that the quantum sampler explores only the feasible subspace defined by the domain.

2.4 Generative Circuit Synthesis vs. Higher-Order Latent Hamiltonian Learning

Recent work explores neural circuit synthesis and parameter transfer, where models such as QAOA-GPT [19], Graph Attention Networks [36], and quantum transformers [32] predict instance-specific

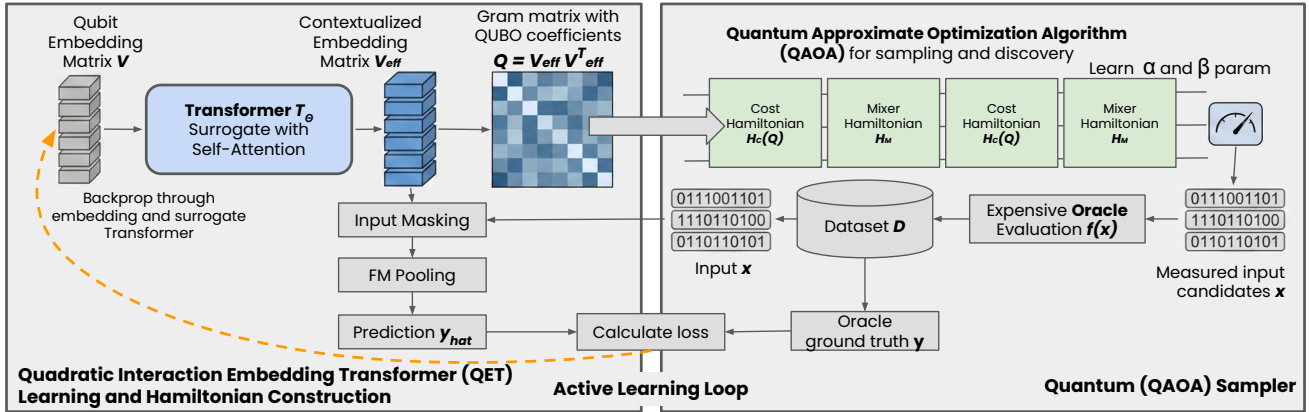


Figure 1: The QET-QAOA Discovery Framework. (A) **Latent-Quadratic Interaction Embedding Transformer:** Contextualizes latent embeddings V via self-attention in Transformer T_θ to capture higher-order dependencies, predicting \hat{y} via Factorization Machine pooling. (B) **QUBO and Hamiltonian Projection:** The learned contextual embeddings V_{eff} forms a Gram matrix $Q = V_{\text{eff}} V_{\text{eff}}^T$, projecting the learned topology onto a valid PSD matrix that defines the QUBO coefficients, which are mapped to an equivalent Ising Hamiltonian H_C . (C) **QAOA Sampling:** This proxy H_C drives a QAOA circuit to sample diverse high-quality configurations, which are evaluated by the Oracle and fed back to iteratively refine the surrogate.

QAOA parameters (γ, β) . Complementarily, dynamic ansatz methods like ADAPT-QAOA [38] grow circuits by selecting operators via energy gradients, achieving strong performance on NISQ devices. These approaches assume that the problem graph (the Hamiltonian H_C) is *known a priori* (e.g., MaxCut on a provided graph). They learn the mapping $\mathcal{G} \rightarrow \text{Circuit}$. In contrast, our work addresses and operates under a *black-box setting* where the underlying interaction graph is unknown and must be inferred from limited data. Our QET architecture performs *Quadratic Structure Learning* ($\text{Data} \rightarrow \mathcal{G}$), effectively serving as the necessary precursor step that makes quantum optimization applicable to black-box tasks.

Finally, while recent works have explored higher-order (HUBO) formulations for portfolio optimization [33] and proposed native multi-body pulses via Digital-Analog Quantum Computing (DAQC) [23], we explicitly constrain our architecture to the Ising model. Implementing native higher-order gates (e.g., ZZZ) requires costly circuit decompositions that limit scalability on Near-Term (NISQ) devices. By using a Transformer to capture higher-order dependencies in the *embedding space* and projecting them onto a quadratic form, QET captures the effective spectral influence of complex interactions without incurring the hardware overhead of a full HUBO implementation.

3 Methodology

Figure 1 illustrates the end-to-end QET-QAOA workflow, which iterates through three phases: (A) learning a latent structural embedding of Latent-Quadratic Interactions from data, (B) projecting these embeddings into a valid Cost Hamiltonian to QAOA, and (C) utilizing the induced quantum energy landscape for diversity sampling.

3.1 Latent-Quadratic Interaction Embedding

3.1.1 Surrogate Modeling: To enable the use of QUBO/Ising Hamiltonian inside QAOA, we first need to approximate the black-box risk function $f(\mathbf{x})$ into a quadratic model. The Latent-Quadratic Interaction Embedding Transformer (QET) model is built upon a global learnable latent matrix $V \in \mathbb{R}^{d \times k}$ comprising individual Latent-Quadratic interactive information as a vector or embedding.

1. Embedding Contextualization: To capture higher-order dependencies, the matrix V is processed by a Transformer encoder T_θ . The self-attention mechanism contextualizes the latent vectors based on their global relationships, outputting a refined matrix $V_{\text{eff}} = T_\theta(V)$.

2. Masked Pooling and Prediction: The input bitstring \mathbf{x} acts as a *masking operator*. The scalar risk score \hat{y} is then computed using the efficient linear-time factorization of the pairwise interactions using a second-order Factorization Machine (FM) pooling layer as given in [26]:

$$\hat{y}(\mathbf{x}) = w_0 + \sum_{i=1}^d w_i x_i + \frac{1}{2} \sum_{f=1}^k \left[\left(\sum_{i=1}^d v_{i,f} x_i \right)^2 - \sum_{i=1}^d (v_{i,f} x_i)^2 \right] \quad (1)$$

Here, the inner term computes the interactions by subtracting the sum of squared elements from the square of the sum of elements, allowing the model to capture all $O(d^2)$ pairwise interactions in just $O(dk)$ time. Here, f represents the index over the embedding dimensions, ranging from 1 to k . The term $v_{i,f}$ denotes the f -th component of the masked latent vector for variable i . This formulation is fully differentiable. During the learning phase, the error signal from the prediction \hat{y} backpropagates through the pooling layer and the Transformer encoder T_θ , updating both the attention weights and the initial latent embeddings V . The entire architecture is trained end-to-end to minimize the Mean Squared Error (MSE) $\mathcal{L} = \frac{1}{N} \sum (y_{\text{true}} - \hat{y})^2$, on the history of observed configurations.

3.1.2 Hamiltonian Extraction. Post-training, we extract the effective latent matrix V_{eff} . The QUBO interaction matrix Q is constructed as the Gram matrix of these refined vectors, which projects the learned problem surface onto a quadratic form:

$$Q = V_{\text{eff}} V_{\text{eff}}^T \quad (2)$$

3.2 Quantum-Assisted Sampling via QAOA

We utilize the Quantum Approximate Optimization Algorithm (QAOA) [4] as a *diversity inducing sampler* instead of a conventional solver by using a low circuit depth $p = 2$ and preparing a wavefunction $|\psi(\gamma, \beta)\rangle$ concentrated on low-energy basins.

3.2.1 Cost Hamiltonian Construction. First, we map the learned QUBO matrix Q to an Ising Hamiltonian H_C using the transformation $x_i \rightarrow (1 - Z_i)/2$. This defines the problem landscape:

$$H_C = \sum_{i < j} J_{ij} Z_i Z_j + \sum_i h_i Z_i \quad (3)$$

J_{ij} and h_i are derived directly from the projected Gram matrix Q .

3.2.2 Topology-Aware Mixing Strategies. An additional component of our framework is the choice of the Mixer Hamiltonian H_M , which governs how the quantum state explores the search space. To leverage the structural information captured by QET, we investigate two distinct mixing strategies:

- (1) **Standard Transverse Mixer (QAOA):** The conventional approach using independent bit-flip operators, $H_M = \sum_i X_i$. This promotes global, unconstrained exploration but ignores variable dependencies.
- (2) **Correlated Mixer (QAOA-Corr):** We propose a structure-aware mixer aligned with the QAOA+ framework [10]. We identify the set of strongest pairwise dependencies \mathcal{E}_{top} from the learned matrix Q (i.e., pairs (i, j) with the largest $|Q_{ij}|$). The mixer is augmented with correlated flip terms:

$$H_M^{\text{corr}} = \sum_i X_i + \lambda \sum_{(i,j) \in \mathcal{E}_{\text{top}}} X_i X_j \quad (4)$$

By including the $X_i X_j$ terms, this operator induces *correlated bit flips*, allowing the sampler to tunnel more effectively through the rugged landscape defined by strong variable interactions.

3.2.3 Execution and Sampling. The circuit evolves the initial state $|+\rangle^{\otimes d}$ by alternating applications of the cost and mixer unitaries p times:

$$|\psi(\gamma, \beta)\rangle = \prod_{l=1}^p e^{-i\beta_l H_M} e^{-i\gamma_l H_C} |+\rangle^{\otimes d} \quad (5)$$

Repeated measurement of the final state yields a batch of candidates that are evaluated by the oracle to obtain their true risk scores. The training dataset \mathcal{D} is then updated via $\mathcal{D} \leftarrow \mathcal{D} \cup \{(\mathbf{x}_i, y_i)\}_{i=1}^B$, where B is the budget size, closing the iterative discovery loop.

3.3 Theoretical Properties

3.3.1 Spectral Validity (PSD Constraint). The parameterization $Q = V_{\text{eff}} V_{\text{eff}}^T$ enforces a rigid geometric constraint whereby the interaction matrix is guaranteed to be Positive Semi-Definite (PSD). For any vector \mathbf{z} , the energy $\mathbf{z}^T Q \mathbf{z} = \|V_{\text{eff}}^T \mathbf{z}\|^2 \geq 0$. This ensures a

Algorithm 1 QET-QAOA Surrogate-Guided Discovery

Require: Budget B , Oracle $f(\cdot)$, QET model \mathcal{M}_θ , QAOA with H_C Cost and H_M Mixer Hamiltonian

- 1: Initialize dataset $\mathcal{D} \leftarrow$ Random Design of Experiments
- 2: **for** $t = |\mathcal{D}|$ to B **do**
- 3: **1. Latent-Quadratic Interaction Embedding Learning:** Train QET \mathcal{M}_θ on \mathcal{D} through FM projection to refine embeddings V
- 4: **2. Hamiltonian Projection:** Compute Gram matrix $Q \leftarrow VV^T$ to form PSD proxy Hamiltonian H_C
- 5: **3. Quantum Parameter Learning:** Optimize QAOA ansatz parameters (γ, β) to minimize $\langle H_C \rangle$ and $\langle H_M \rangle$
- 6: **4. Sampling:** Measure the wavefunction $|\psi(\gamma, \beta)\rangle$ to sample diverse batch $\{\mathbf{x}'_1, \dots, \mathbf{x}'_k\}$
- 7: **5. Oracle Evaluation:** Query $y'_i = f(\mathbf{x}'_i)$ for top-k candidates in batch
- 8: **6. Active Update:** $\mathcal{D} \leftarrow \mathcal{D} \cup \{(\mathbf{x}'_i, y'_i)\}$
- 9: **end for**
- 10: **return** Discovery Archive \mathcal{D}

smooth, convex-like energy surface, preventing the *shattered* landscapes [27] (indefinite matrices with many saddle points) that often plague unconstrained polynomial regression.

3.3.2 Implicit Projection of Higher-Order Terms. While the true function $f(\mathbf{x})$ contains higher-order interactions $(x_i x_j x_k)$, QET performs a *learned variational projection*. Formally, minimizing the MSE objective is equivalent to projecting the true higher-order risk function onto the manifold of Ising models, finding the closest pairwise approximation supported by the data [21]. By training QET to minimize MSE, the model learns a latent configuration V_{eff} that best approximates the marginal contribution of these higher-order terms. Consequently, the pairwise term $Q_{ij} = \langle \mathbf{v}'_i, \mathbf{v}'_j \rangle$ encodes the effective conditional influence of third-party variables, projecting the complex risk surface onto an optimal Ising basis without requiring auxiliary qubits [15].

3.4 Quantifying Discovery: Set-Theoretic Exclusivity

To formally evaluate the *marginal contribution* of the quantum sampler, we introduce the Exclusive Yield metric. Let S_Q be the set of high-utility solutions found by our framework, and $S_{\text{Classical}}$ be the union of solutions found by all other classical baselines. The *Exclusive Yield* (η_{ex}) is defined as:

$$\eta_{\text{ex}}(Q) = \frac{|S_Q \setminus S_{\text{Classical}}|}{|S_Q \cup S_{\text{Classical}}|} \quad (6)$$

This metric rigorously quantifies the proportion of the high-utility landscape that is accessible *solely* via the quantum-assisted approach.

4 Experimental Evaluation

We evaluate the proposed QET-QAOA framework against a comprehensive suite of 10 state-of-the-art baselines with variants. The primary objective is to validate how well quantum methods and the learned QET surrogate in particular effectively capture the complex

problem landscape, enabling samplers to recover high-utility configurations accessible to standard heuristics. Our analysis is guided by two refined research questions: **RQ1 (Comparative Discovery):** How do quantum-guided methods using FM and QET surrogates compare against state-of-the-art evolutionary, Bayesian, and reinforcement learning baselines in discovering high-risk configurations under strict evaluation budgets, when all methods operate under identical oracle constraints? **RQ2 (Surrogate Ablation):** Does the Latent-Quadratic Interaction Embedding Transformer (QET) provide a measurable advantage over standard Factorization Machines (FM) in a controlled ablation study where the surrogate model is the only varying component?

4.1 Case Study: Discovering Risky Documents in IDP Pipeline Evaluation

To simulate a realistic, high-dimensional black-box optimization task, we utilize an Enterprise Intelligent Document Processing (IDP) pipeline described in [7]. The optimization goal is *Risk Document Discovery*: finding valid binary configurations $\mathbf{x} \in \{0, 1\}^d$ that generate synthetic documents maximizing the failure rate of downstream OCR and extraction models. Each configuration specifies a structured document blueprint via binary-encoded structural parameters such as table density, noise artifacts, pagination behavior, and layout variations, which we refer to as *risk features*. We consider two complexity regimes: (i) *Single-Page Regime* ($d = 24$), capturing lower-order interactions (e.g., local layout shifts, font noise), and (ii) *Multi-Page Regime* ($d = 27$), introducing higher-order dependencies such as cross-page table consistency and split layouts. The oracle function $f(\mathbf{x})$ returns a scalar risk score computed as the aggregate error of the IDP pipeline across OCR accuracy, layout analysis, table structure recognition, and key-value extraction correctness, with each evaluation requiring a full document generation and end-to-end pipeline execution.

4.2 Baseline Algorithms

We compare QET-QAOA against representative solvers from four major optimization families. All methods use standard libraries and identical hyperparameters where applicable.

Evolutionary and Swarm (Population-Based): Genetic Algorithms (GA) implemented in DEAP, including an exploration-biased variant (high mutation, $p_m = 0.1$) and an exploitation-biased variant (high crossover, $p_c = 0.9$); and Particle Swarm Optimization (PSO) using a binary PSO implementation (pyswarms) with inertia weight $w = 0.7$.

Quality-Diversity (QD): MAP-Elites implemented using ribs, maintaining a 25×25 feature grid to enforce diversity and serve as the primary coverage-oriented baseline.

Bayesian Optimization (Surrogate-Based): GP-EI and GP-UCB using Gaussian Process surrogates from scikit-learn, and TPE (Tree-structured Parzen Estimator) implemented in Optuna for discrete search spaces.

Reinforcement Learning (Policy Gradient): PPO and REINFORCE implemented in Stable-Baselines3, trained to maximize risk reward; PPO-Div additionally incorporates entropy regularization (coefficient = 0.03) to promote exploration.

4.3 Quantum Implementation

QET-QAOA is implemented as follows: *Surrogate Model (QET)*: A Latent-Quadratic Interaction Embedding Transformer in torch with 2 self-attention layers (4 heads, hidden dim=16 each) is trained via Adam with learning rate of 0.001 with weight decay of 1e-4 for 500 steps. We compare this against FM as surrogates. *Circuit Ansatz*: We utilize a QAOA circuit of depth $p = 2$, using the PennyLane framework with the lightning.kokkos backend. Variational parameters (γ, β) are optimized via COBYLA for 500 iterations per sampling step. We evaluate two mixing Hamiltonians: (i) *Standard Mixer (QAOA)*: $H_M = \sum_i X_i$ (Induces independent bit flips), (ii) *Correlated Mixer (QAOA-Corr)*: $H_M = \sum_i X_i + \lambda \sum_{(i,j) \in \mathcal{E}} X_i X_j$, utilizing the top-k strong interactions from Q to induce structured transitions.

4.4 Implementation Details

Each method is evaluated with a limited budget of $B = 1000$ oracle calls to simulate a constrained evaluation environment. All surrogate and learning-based methods use the same random initial design comprising $N_{\text{init}} = 100$ configurations. At each iteration, 50 samples are selected or generated by each method. The average scores across 3 seeds are reported in quantitative results.

4.5 Comparative Efficacy

Table 1 illustrates the performance of Quantum-assisted solvers relative to classical baselines across two complexity regimes.

4.5.1 Exploitation vs Exploration: We compare how good each method is in finding not only high risks (optimize) but also diversify (sample), by comparing across the max, mean, std.dev. risk scores. In the 24D regime, classical baselines like PPO-Div (4.40), TPE (4.30), and GP-EI (4.23) excel at climbing local gradients. However, their success is brittle. The $T10\sigma$ (Std. Dev of Top-10%) metric reveals a critical flaw: GA-Exploit, SA, and TPE all show near-zero variance (≤ 0.05). This indicates they converge to a *single* failure mode and repeatedly resample it. In contrast, Quantum methods like QET-QAOA (4.29) exhibits both competitive max score and also variance; QET-QAOA-Corr maintains a $T10\sigma$ of 0.37 (24D) and 0.39 (27D). Even while achieving the second-highest overall Max Risk (5.54), the σ is relatively higher. This shows the quantum sampler is effectively exploring not just the single most top value, but multiple distinct basins simultaneously, a property unique to quantum superposition.

4.5.2 Topological Exclusivity versus all other methods: To understand the unique exploratory capabilities of each search strategy, we perform a pairwise analysis of the core risk modes discovered by each method at the end of its budget. We consider the discovery aspect through set-theoretic exclusivity, as described in Section 3.4. In the 24D setting, several classical methods already achieve substantial unique layout discovery and high exclusivity (e.g., GP at 7.7% and REINFORCE at 7.5%), which narrows the relative exclusivity gains of quantum-based methods. However, in 27D its low exclusivity (3.3%) suggests it might be harder to identify newer configurations with increase in dimensionality. MAP-Elites (9.0%) and PSO (7.7%) lead in exclusivity in 27D, suggesting simpler diversity-driven objectives might have better reach in high dimensions with constrained budgets. QAOA-Corr methods (FM 5.4% and QET 5.3%)

Table 1: Comprehensive performance metrics under fixed budget $B = 1000$ (Mean of 3 seeds). Max: Best risk score. $T10\mu/\sigma$: Mean/Std.Dev of Top-10% solutions. UL: Unique high-risk configurations. Ex%: Exclusive Yield. Bold=Best, Underline=Second Best (among solvers). Random sampling is given for baseline reference and is not considered for results analysis.

Class	Method	Single-Page Regime (24D)						Multi-Page Regime (27D)					
		Max	Mean	$T10\mu$	$T10\sigma$	UL	Ex%	Max	Mean	$T10\mu$	$T10\sigma$	UL	Ex%
Local	Random	4.09	2.33	3.49	0.23	860	10.9	4.68	2.36	3.65	0.28	981	12.1
	SA	3.98	2.97	3.96	0.02	209	0.7	4.65	3.50	4.47	0.04	292	1.2
Evol	GA-Explore	4.10	3.25	4.10	0.05	378	3.2	5.06	3.81	4.54	0.12	325	2.1
	GA-Exploit	4.13	3.73	4.07	0.01	109	0.4	4.50	4.25	4.50	0.00	102	0.5
	PSO	3.92	2.32	3.61	0.12	341	2.6	5.75	2.55	4.10	<u>0.39</u>	614	<u>7.7</u>
QD	MAP-Elites	4.14	2.46	3.56	0.18	466	5.1	4.71	2.69	4.07	0.19	671	9.0
	GP-EI	4.23	3.07	3.87	0.12	957	7.7	5.32	3.41	4.33	0.28	994	3.3
Bayes	GP-UCB	4.18	3.11	3.85	0.09	957	<u>7.6</u>	5.15	3.43	4.33	0.22	<u>993</u>	3.3
	TPE	<u>4.30</u>	3.47	3.96	0.03	187	1.2	4.44	3.94	4.44	0.00	242	2.1
RL	REINFORCE	4.18	2.33	3.71	0.13	809	7.5	5.16	2.81	4.29	0.18	850	6.8
	PPO-Div	4.40	2.87	3.85	0.15	687	4.7	4.92	3.21	4.41	0.16	724	5.0
	PPO-Risk	4.30	3.04	3.84	0.11	568	3.5	5.30	3.48	<u>4.52</u>	0.15	560	3.3
QAOA	FM-QAOA	4.13	2.66	3.84	0.11	651	3.6	4.91	3.12	4.44	0.15	701	4.6
	FM-QAOA-Corr	3.99	2.37	3.73	0.12	744	5.1	4.76	2.82	4.22	0.19	761	5.4
	QET-QAOA	4.29	2.05	3.16	0.37	462	3.8	4.67	2.35	3.89	0.34	679	4.9
	QET-QAOA-Corr	4.10	2.01	3.18	0.37	520	4.4	<u>5.54</u>	2.42	3.85	0.39	711	5.3

remain competitive in this tier, outperforming all other evolutionary and Bayesian methods. This indicates that the correlated mixer is able to sample the search subspace relatively better than gradient-based manifolds in higher dimensions.

4.5.3 Pairwise Exclusivity of Core Risk Structures: To differentiate amongst minor configuration variants, we define *core risk modes* by collapsing failures to their essential semantic predicates (failure type, density regime, noise regime, and layout interaction), creating a set of fundamental structural properties

Tables 2 and 3 report pairwise exclusivity of *core risk modes* in the 24D and 27D regimes, respectively, quantifying shared and solver-specific discoveries across methods.

24D (Single-Page Regime). In the lower-dimensional setting, quantum-guided methods consistently outperform classical baselines in exclusive core mode discovery. In particular, QET-QAOA with a correlated mixer (QET-C) acts as a near-superset of most classical solvers, discovering multiple core modes missed by BO methods (e.g., GP-EI, TPE), Simulated Annealing, and MAP-Elites, while rarely missing modes found by them. Among quantum variants, both the QET surrogate and correlated mixing systematically improve exclusivity, indicating that modeling higher-order interactions enables traversal across energy barriers that trap local or purely stochastic search strategies.

27D (Multi-Page Regime). In the higher-dimensional setting, MAP-Elites achieves the strongest exclusivity across most pairwise comparisons, consistent with the scalability of archive-based illumination under increasing combinatorial complexity. Nevertheless, QET-QAOA remains competitive, often ranking second and consistently outperforming BO and RL baselines. The advantage of correlated quantum mixers diminishes in this regime, suggesting that reliable estimation of higher-order correlations requires more data as dimensionality increases.

Overall, the pairwise analysis confirms that no single solver dominates across regimes: MAP-Elites excels in high-dimensional

Table 2: Comparing pairwise mode exclusivity for 24D (Single Page). Format: Shared / Row_{Excl} / Col_{Excl}. To read col-wise: Green if Col > Row, Red if Row > Col, Orange if Col = Row.

Method	GP-EI	MAP-E	PPO	QET	FM	QET-C	FM-C	SA
GP-EI	—	18/6/1	21/3/3	23/1/1	24/0/1	24/0/3	24/0/2	21/3/0
MAP-E	18/1/6	—	19/0/5	19/0/5	18/1/7	19/0/8	19/0/7	15/4/6
PPO	21/3/3	19/5/0	—	21/3/3	22/2/3	24/0/3	23/1/3	18/6/3
QET-QAOA	23/1/1	19/5/0	21/3/3	—	23/2/1	24/0/3	24/0/2	20/4/1
FM-QAOA	24/1/0	18/7/1	22/3/2	23/1/2	—	25/0/2	25/1/0	21/4/0
QET-Corr	24/3/0	19/8/0	24/3/0	24/3/0	25/2/0	—	26/1/0	21/6/0
FM-Corr	24/2/0	19/7/0	23/3/1	24/2/0	25/0/1	26/0/1	—	21/5/0
SA	21/0/3	15/6/4	18/3/6	20/1/4	21/0/4	21/0/6	21/0/5	—

Table 3: Comparing pairwise mode exclusivity for 27D (Multi Page). Format: Shared / Row_{Excl} / Col_{Excl}. To read col-wise: Green if Col > Row, Red if Row > Col, Orange if Col = Row.

Method	GP-EI	MAP-E	PPO	QET	FM	QET-C	FM-C	SA
GP-EI	—	37/3/7	33/7/4	36/4/5	36/3/4	32/8/4	37/3/2	33/7/0
MAP-E	37/7/3	—	35/9/2	38/6/3	36/8/3	33/11/3	36/8/3	30/14/3
PPO	33/4/7	35/2/9	—	35/2/6	35/2/4	30/7/6	34/3/5	29/8/4
QET-QAOA	36/5/4	38/3/6	35/6/2	—	37/4/2	35/6/1	36/5/3	33/8/0
FM-QAOA	36/3/4	36/3/8	35/4/2	37/2/4	—	34/5/2	37/2/2	33/6/0
QET-Corr	32/4/8	33/3/11	30/6/7	35/1/6	34/2/5	—	33/3/6	32/4/1
FM-Corr	37/2/3	36/3/8	34/5/3	36/3/5	37/2/2	33/6/3	—	33/6/0
SA	33/0/7	30/3/14	29/4/8	33/0/8	33/0/6	32/1/4	33/0/6	—

illumination, while quantum-guided methods provide complementary discovery capabilities by uncovering exclusive core risk modes missed by classical optimizers.

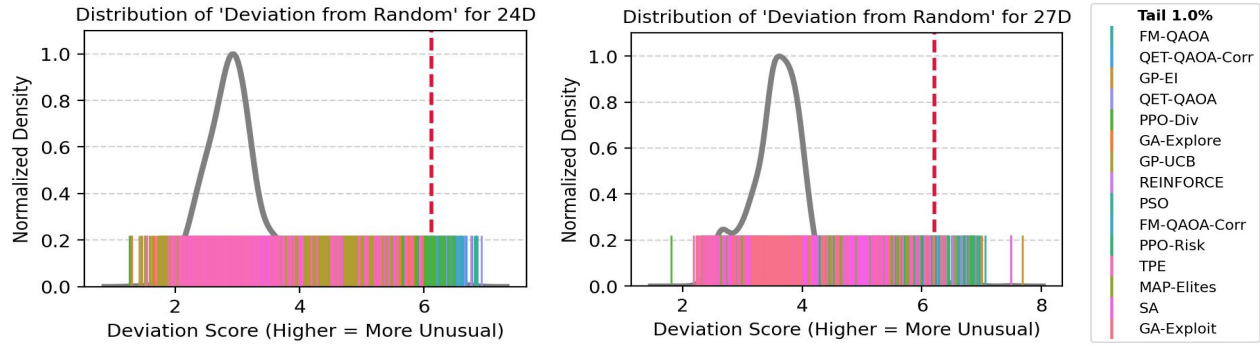


Figure 2: Tail distribution plot across all methods, for 24D and 27D regimes.

4.5.4 Distributional Tail Sampling: While exclusive discovery captures *what* failures are found, effective stress testing also requires measuring *tail diversity*: the ability to discover structurally extreme configurations far from typical solutions. We quantify structural atypicality using a deviation score, defined as the standardized Euclidean distance from a random-sampled centroid in configuration space. Table 4 reports the number of configurations falling within the top 1% of this deviation distribution, while Figure 2 shows the full deviation-score distributions.

Table 4: Distributional Tail Sampling. Number of configurations discovered within the 1% structural deviation tail, out of 1000 samples per method.

Method	24D Tail (1%)	27D Tail (1%)
FM-QAOA-Corr	27	18
FM-QAOA	12	26
QET-QAOA-Corr	23	21
QET-QAOA	20	14
MAP-Elites	18	2
REINFORCE	16	13
PPO-Risk	12	7
GP-EI	0	12
GP-UCB	0	10
GA-Explore	0	10
TPE	0	3
SA	0	2
GA-Exploit	0	1

Two clear patterns emerge. First, several objective-driven optimizers with strong average performance contribute few or no tail elites in the 24D regime, indicating concentration around dominant risk structures. While diversity-oriented MAP-Elites improves tail coverage, it remains below the best quantum methods. Second, QAOA-based samplers consistently rank at or near the top in tail discovery across both dimensions, for example, FM-QAOA-Corr in 24D and FM-QAOA in 27D, with QET-QAOA-Corr remaining consistently competitive, demonstrating more reliable recovery of structurally extreme risk configurations. Figure 2 illustrates the underlying mechanism. Classical optimizers concentrate sampling

mass near central, frequently visited structures, whereas surrogate-guided QAOA maintains heavier distributional tails. Because QAOA samples from a learned energy-shaped distribution rather than iteratively collapsing toward a single improving mode, multiple high-risk basins, including structurally distant ones, retain non-negligible probability mass under fixed evaluation budgets.

4.5.5 Surrogate Generalizability & Information Gain. Beyond immediate risk discovery, a critical property of a search strategy is the information value of the samples it generates. Does the solver explore the landscape informatively, producing data that allows a model to generalize to unseen regions? This reframes the problem to asking which solver generates the best training data for mapping the global risk function? To quantify this, we treat the sample history of each solver ($N = 700$) as a training set for a Random Forest Regressor and evaluate its predictive accuracy (R^2) on the remaining 30% from each method to form the collective global hold-out validation set.

The results in Table 5 demonstrate the superior information gain of the quantum-guided search: **Quality over Quantity**: In the 24D regime, the model trained on data from QET-QAOA-Corr achieves the highest generalization score ($R^2 = 0.840$), significantly outperforming models trained on RL (0.78%), GP-EI ($R^2 = 0.652$) or TPE ($R^2 = 0.658$). This implies that the quantum sampler covers the landscape's geometry more comprehensively compared to other methods. **Robustness**: While GP-EI performs well in 27D ($R^2 = 0.757$), FM-QAOA (0.741) and QET-QAOA (0.740) remain statistically equivalent. While Gaussian Process (GPs) suffer from cubic computational complexity ($O(N^3)$) [25] with respect to the number of samples, our parametric QET transformer surrogate reduces this to quadratic complexity ($O(N^2)$) (with scope to be further brought down to $(O(N))$ using linear attention [14]), enabling efficient learning in high-dimensional spaces where traditional Bayesian Optimization becomes computationally prohibitive.

4.6 Architectural Ablation (QET vs. FM)

We compare the Latent-Quadratic Embedding Transformer (QET) and Factorization Machine (FM) surrogates under identical data, training budgets, and QAOA settings. Both produce quadratic surrogate Hamiltonians; they differ only in interaction modeling: FM

Table 5: Surrogate Generalizability (R^2). Models are trained **only on 70% of samples discovered by each specific method, and tested on the hold-out 30% validation.** A higher R^2 indicates the method explored the landscape more informatively, finding samples across regions leading to generalization.

Training Source	24D			27D		
	$R^2 \uparrow$	$MAE \downarrow$	MAPE	$R^2 \uparrow$	$MAE \downarrow$	MAPE
Reference (All Data)	0.924	0.157	0.068	0.924	0.174	0.064
QET-QAOA-Corr	0.840	0.269	0.107	0.729	0.374	0.152
FM-QAOA-Corr	0.824	0.279	0.123	0.726	0.369	0.147
QET-QAOA	0.798	0.293	0.120	0.740	0.388	0.135
FM-QAOA	0.785	0.299	0.140	0.741	0.386	0.146
REINFORCE	0.787	0.297	0.117	0.719	0.365	0.123
PPO-Div	0.781	0.305	0.146	0.712	0.378	0.131
GP-EI	0.652	0.364	0.216	0.757	0.350	0.158
MAP-Elites	0.681	0.376	0.193	0.573	0.478	0.166
TPE	0.658	0.376	0.211	0.652	0.441	0.175
Random	0.679	0.332	0.197	0.510	0.502	0.179

encodes explicit pairwise terms, whereas QET captures higher-order dependencies via contextual self-attention before quadratic projection.

Surrogate fidelity: Predictive accuracy is comparable across regimes (Table 5). In 24D, QET generalizes slightly better ($R^2 = 0.840$ vs. 0.824), while in 27D both achieve similar performance ($R^2 \approx 0.73 - 0.74$), indicating that downstream differences are not driven by prediction error.

Induced search behavior: Despite similar fidelity, the induced QAOA sampling distributions differ. In 24D, where interactions are mostly pairwise, FM provides broader coverage and higher mean sampled risk (UL: 744 vs. 462), while QET reaches higher-risk extremes (max: 4.29 vs. 4.13/3.99). In 27D, FM maintains larger coverage (UL: 761 vs. 272), whereas QET accesses substantially higher extremes (max: 5.54 vs. 4.76), consistent with sensitivity to higher-order interactions.

Elite diversity: QET consistently produces more structurally diverse elites (Top-10% variance: 0.37/0.39 vs. FM 0.11/0.19), indicating that contextual interaction modeling reshapes the quadratic energy landscape so that multiple high-risk basins remain competitive. Overall, FM favors broad coverage through pairwise averaging, whereas QET favors selective extreme discovery and elite diversity, with advantages increasing as interaction complexity grows.

5 Discussion

We study diversity-oriented discovery under strict query budgets, where the objective is to recover a diverse set of high-utility configurations rather than a single optimum. In this black-box regime, surrogate-guided quantum sampling is effective: learning a quadratic proxy and sampling with QAOA shifts search behavior from mode-seeking optimization toward distributional exploration. Discovery behavior is primarily governed by mixer topology and circuit depth. Interaction-aware correlated mixers improve connectivity between high-utility regions and increase exclusive discovery in structured settings. For sampling, shallow circuits are preferable,

as they preserve probability mass across multiple basins, whereas deeper circuits tend to over-concentrate on a few optima, reducing diversity and increasing cost. Surrogate structure determines which regions of the landscape are amplified. Pairwise surrogates are effective when interactions are simple, but saturate as dimensionality and interaction complexity grow. Contextual surrogates that model higher-order dependencies before quadratic projection reshape the geometry of the learned energy landscape, altering the induced sampling distribution even when predictive accuracy is comparable. Compared to classical optimizers, which often collapse to dominant modes, surrogate-guided QAOA maintains heavier distributional tails and improves exclusive discovery. The FM–QET ablation reveals a regime-dependent trade-off: pairwise surrogates favor broad coverage, while contextual surrogates improve tail discovery and diversity when higher-order structure is present.

6 Conclusion

This work presents a surrogate-guided quantum sampling framework that learns interaction-aware quadratic proxy Hamiltonians from data by projecting higher-order dependencies, captured via a Transformer-based Latent-Quadratic Interaction embedding, into QAOA-compatible forms. Using shallow-depth QAOA, the framework enables diversity-oriented discovery under strict evaluation budgets, improving tail discovery, elite diversity, and exclusivity relative to classical baselines while remaining hardware-efficient. Beyond quantum sampling, QET-style contextual surrogate construction functions as a learned QUBO feature map that lifts structured inputs into interaction-aware quadratic representations, making them compatible with both quantum algorithms and classical optimizers. This enables reuse in surrogate-assisted combinatorial optimization and black-box search. Promising directions include transferring learned embeddings across related tasks, and integrating the surrogate as a plug-in to extend the framework to constrained and multi-objective optimization settings.

Acknowledgments

This work is supported by PhiLabs, Quantiphi. We would like to thank Varun V for suggesting editorial improvements to the manuscript, Harkrishnan PM for inputs on the IDP pipeline, and our cofounder Asif Hasan for the continued support.

References

[1] James Bergstra, Rémi Bardenet, Yoshua Bengio, and Balázs Kégl. 2011. Algorithms for Hyper-parameter Optimization. In *Advances in Neural Information Processing Systems*, J. Shawe-Taylor, R. Zemel, P. Bartlett, F. Pereira, and K. Q. Weinberger (Eds.), Vol. 24. Curran Associates, Inc., 2546–2554. <https://proceedings.neurips.cc>

[2] Matej Črepinsek, Shih-Hsi Liu, and Marjan Mernik. 2013. Exploration and exploitation in evolutionary algorithms: A survey. *ACM Computing Surveys (CSUR)* 45, 3 (2013), 1–33.

[3] Leyang Cui, Yiheng Xu, Tengchao Lv, and Furu Wei. 2021. Document AI: Benchmarks, Models and Applications. *arXiv preprint arXiv:2111.08609* (2021).

[4] Edward Farhi, Jeffrey Goldstone, and Sam Gutmann. 2014. A quantum approximate optimization algorithm. *arXiv preprint arXiv:1411.4028* (2014).

[5] Paul Glasserman. 2004. *Monte Carlo Methods in Financial Engineering*. Stochastic Modelling and Applied Probability, Vol. 53. Springer Science & Business Media, New York, NY. doi:10.1007/978-0-387-21617-1

[6] Rafael Gómez-Bombarelli, Jennifer N Wei, David Duvenaud, José Miguel Hernández-Lobato, Benjamín Sánchez-Lengeling, Dennis Sheberla, Jorge Aguilera-Iparraguirre, Timothy D Hirzel, Ryan P Adams, and Alán Aspuru-Guzik. 2018. Automatic chemical design using a data-driven continuous representation of molecules. *ACS central science* 4, 2 (2018), 268–276.

[7] Saisubramaniam Gopalakrishnan, Dagnachew Birru, et al. 2026. Search-Based Risk Feature Discovery in Document Structure Spaces under a Constrained Budget. *arXiv preprint arXiv:2601.21608* (2026).

[8] Sudipto Guha and Kamesh Munagala. 2007. Approximation Algorithms for Budgeted Learning Problems. In *Proceedings of the 39th Annual ACM Symposium on Theory of Computing*. 104–113.

[9] Huirong Guo, Ruiming Tang, Yunming Ye, Zhenguo Li, and Xiuqiang He. 2017. DeepFM: A Factorization-Machine based Neural Network for CTR Prediction. In *Proceedings of the 26th International Joint Conference on Artificial Intelligence (IJCAI)*. 1725–1731. doi:10.24963/ijcai.2017/239

[10] Stuart Hadfield, Zhihui Wang, Bryan O’Gorman, Eleanor G Rieffel, Davide Venturelli, and Rupak Biswas. 2019. From the quantum approximate optimization algorithm to a quantum alternating operator ansatz. *Algorithms* 12, 2 (2019), 34.

[11] John H Holland. 1975. *Adaptation in natural and artificial systems: an introductory analysis with applications to biology, control, and artificial intelligence*. University of Michigan Press.

[12] Sanghyo Hwang, Seongmin Kim, Zhihua Xu, Tengfei Luo, and Eungkyu Lee. 2025. Higher-order factorization machine for accurate surrogate modeling in material design. *Scientific Reports* 15, 1 (2025), 19270. doi:10.1038/s41598-025-19270-6

[13] Tadashi Kadokawa and Hidetoshi Nishimori. 1998. Quantum annealing in the transverse Ising model. *Physical Review E* 58, 5 (1998), 5355–5363.

[14] Angelos Katharopoulos, Apoorv Vyas, Nikolaos Pappas, and François Fleuret. 2020. Transformers are RNNs: Fast Autoregressive Transformers with Linear Attention. In *Proceedings of the 37th International Conference on Machine Learning (ICML)*. PMLR, 5156–5165. <https://proceedings.mlr.press>

[15] Julia Kempe, Alexei Kitaev, and Oded Regev. 2006. The Complexity of the Local Hamiltonian Problem. *SIAM J. Comput.* 35, 5 (2006), 1070–1097. doi:10.1137/S009753970444522X

[16] James Kennedy and Russell Eberhart. 1995. Particle swarm optimization. In *Proceedings of ICNN’95-International Conference on Neural Networks*, Vol. 4. IEEE, 1942–1948. doi:10.1109/ICNN.1995.488968

[17] Koki Kitai, Jiang Guo, Shenghong Ju, Shu Tanaka, Koji Tsuda, Junichiro Shiomi, and Ryo Tamura. 2020. Designing metamaterials with quantum annealing and factorization machines. *Physical Review Research* 2, 1 (2020), 013319.

[18] Joel Lehman and Kenneth O Stanley. 2011. Evolving a diversity of virtual creatures through novelty search and local competition. In *Proceedings of the 13th annual conference on Genetic and evolutionary computation*. 211–218.

[19] Runze Mao et al. 2025. Extending QAOA-GPT to Higher-Order Quantum Optimization Problems. *arXiv preprint arXiv:2511.07391* (2025).

[20] Natalie Maus, Haydn Jones, Juston Moore, Matt J Kusner, John Bradshaw, and Jacob Gardner. 2023. Discovering Many Diverse Solutions with Bayesian Optimization. In *Proceedings of the 26th International Conference on Artificial Intelligence and Statistics (AISTATS)*. PMLR, 5969–5996.

[21] Pankaj Mehta, Marin Bukov, Ching-Hao Wang, Alexandre GR Day, Clint Richardson, Charles K Fisher, and David J Schwab. 2019. A high-bias, low-variance introduction to Machine Learning for physicists. *Physics Reports* 810 (2019), 1–124.

[22] Jean-Baptiste Mouret and Jeff Clune. 2015. Illuminating search spaces by mapping elites. *arXiv preprint arXiv:1504.04909* (2015).

[23] Adrian Parra-Rodríguez, Pavel Lougovski, Lucas Lamata, Enrique Solano, and Mikel Sanz. 2020. Digital-analog quantum computation. *Physical Review A* 101, 2 (2020), 022305. doi:10.1103/PhysRevA.101.022305

[24] Justin K. Pugh, Lisa B. Soros, and Kenneth O. Stanley. 2016. Quality Diversity: A New Frontier for Evolutionary Computation. *Frontiers in Robotics and AI* 3 (2016), 40. doi:10.3389/frobt.2016.00040

[25] Carl Edward Rasmussen and Christopher K. I. Williams. 2006. *Gaussian Processes for Machine Learning*. MIT Press, Cambridge, MA. <http://www.gaussianprocess.org>

[26] Steffen Rendle. 2010. Factorization machines. In *2010 IEEE International Conference on Data Mining*. IEEE, 995–1000. doi:10.1109/ICDM.2010.127

[27] Bernhard Schölkopf and Alexander J. Smola. 2002. *Learning with Kernels: Support Vector Machines, Regularization, Optimization, and Beyond*. MIT Press, Cambridge, MA. <https://mitpress.mit.edu>

[28] John Schulman, Filip Wolski, Prafulla Dhariwal, Alec Radford, and Oleg Klimov. 2017. Proximal policy optimization algorithms. *arXiv preprint arXiv:1707.06347* (2017).

[29] Bobak Shahriari, Kevin Swersky, Ziyu Wang, Ryan P Adams, and Nando De Freitas. 2015. Taking the human out of the loop: A review of bayesian optimization. *Proc. IEEE* 104, 1 (2015), 148–175.

[30] Jasper Snoek, Hugo Larochelle, and Ryan P. Adams. 2012. Practical Bayesian Optimization of Machine Learning Algorithms. In *Advances in Neural Information Processing Systems*, F. Pereira, C.J. Burges, L. Bottou, and K.Q. Weinberger (Eds.), Vol. 25. Curran Associates, Inc., 2951–2959. <https://proceedings.neurips.cc>

[31] Ryo Tamura, Koki Kitai, Takumi Matsumoto, Shinsuke Ju, Junichiro Shiomi, and Koji Tsuda. 2023. Black-box optimization with the D-Wave quantum annealer for material exploration. *Frontiers in Computer Science* 5 (2023), 1286226. doi:10.3389/fcomp.2023.1286226

[32] Shehbaz Tariq et al. 2025. A Survey of Quantum Transformers: Architectures, Challenges and Outlooks. *arXiv preprint arXiv:2504.03192* (2025).

[33] Valter Uotila, Julia Ripatti, and Bo Zhao. 2025. Higher-Order Portfolio Optimization with Quantum Approximate Optimization Algorithm. In *2025 IEEE International Conference on Quantum Computing and Engineering (QCE)*. IEEE, 1–12. doi:10.1109/QCE65121.2025.00244 Also available as arXiv:2509.01496.

[34] Ronald J Williams. 1992. Simple statistical gradient-following algorithms for connectionist reinforcement learning. *Machine learning* 8, 3 (1992), 229–256.

[35] Jun Xiao, Hao Ye, Xiangnan He, Hanwang Zhang, Fei Wu, and Tat-Seng Chua. 2017. Attentional Factorization Machines: Learning the Weight of Feature Interactions via Attention Networks. In *Proceedings of the 26th International Joint Conference on Artificial Intelligence (IJCAI)*. 3119–3125.

[36] Anqi Zhang et al. 2025. QAOA Parameter Transferability for Maximum Independent Set using Graph Attention Networks. *arXiv preprint arXiv:2504.21135* (2025).

[37] MengChu Zhou, Meiji Cui, Dian Xu, Shuwei Zhu, Ziyuan Zhao, and Abdullah Abusorrah. 2024. Evolutionary Optimization Methods for High-Dimensional Expensive Problems: A Survey. *IEEE/CAA Journal of Automatica Sinica* 11, 5 (2024), 1092–1105. doi:10.1109/JAS.2024.124320

[38] Linghua Zhu, Ho Lun Tang, George S Barron, FA Calderon-Vargas, Nicholas J Mayhall, Edwin Barnes, and Sophia E Economou. 2022. Adaptive quantum approximate optimization algorithm for solving combinatorial problems on a quantum computer. *Physical Review Research* 4, 3 (2022), 033029.